EFFECT OF TPRD DIAMETER AND DIRECTION OF RELEASE ON HYDROGEN DISPERSION IN UNDERGROUND PARKING

V. Shentsov, D. Makarov, V. Molkov
HySAFER, School of the Built Environment, Ulster University, BT37 0QB, UK,
v.shentsov@ulster.ac.uk

ABSTRACT

Unignited hydrogen release in underground parking could be considered inherently safer if the safety strategy to avoid the formation of the flammable hydrogen-air mixture under a ceiling is followed. This strategy excludes destructive deflagrative combustion and associated pressure and thermal effects in the case of ignition. This paper aims at understanding the effects of the thermally activated pressure relieve device (TPRD) diameter and direction of release on the build-up of hydrogen flammable concentration under the ceiling in the presence of mechanical ventilation required for underground parking. The study employs the similarity law for hydrogen jet concentration decay in a free under-expanded jet to find the lower limit of TPRD diameter that excludes the formation of a flammable mixture under the ceiling during upward release. This approach is conservative and does not include the effect of mechanical ventilation providing flow velocity around a few meters per second, which is significantly below velocities in hydrogen momentum-dominated under-expanded jets. Hydrogen releases downwards under a vehicle at different angles and with different air velocities due to mechanical ventilation were investigated using computational fluid dynamics (CFD). The joint effect of TPRD diameter, release direction and mechanical ventilation is studied. TPRD diameters for the release of hydrogen upwards and downwards preventing the creation of flammable hydrogen-air mixture under the parking ceiling are defined for different ceiling heights and locations of TPRD above the floor. Recommendations to the design of TPRD devices to underpin the safe introduction of hydrogen fuelled vehicles in currently existing underground parking and infrastructure are formulated.

KEYWORDS: Hydrogen safety, unignited release, mechanical ventilation, underground parking, TPRD, CFD

1.0 INTRODUCTION

The development of safety strategies to prevent the formation of flammable hydrogen-air composition in underground traffic infrastructure and parking areas is the current topic of interest for safety and design engineers in connection with ever increasing number of fuel cell electric vehicles (FCEV) on public roads. In case of a hydrogen leak in an enclosure, it is recommended to have a ventilation system preventing accumulating of hydrogen concentration above 1% vol. [1–3]. In the context of underground parking, the hydrogen release may originate from an accidentally triggered thermally activated pressure releave device (TPRD), which is a standard safety feature required for onboard storage of every FCEV. Mechanical ventilation currently installed in underground parking areas, controlling air quality and potential fire hazards, is specified by corresponding regulations, codes and standards (RCS), e.g. BS 7346-7 [4]. Interaction of hydrogen releases from TPRD with already installed in underground parking mechanical ventilation is a credible accident scenario.

The effect of mechanical ventilation on hydrogen dispersion in closed spaces was examined in few numerical studies. In 2013 Choi et al. [5] performed numerical simulations of hydrogen release from onboard storage in an underground parking with and without mechanical ventilation. The considered parking had dimensions $W \times L \times H$=18.0×16.7×2.3 m. In simulations with ventilation the parking entrance was wide open, $W \times H$=5.0×2.3 m, with mechanical ventilator located on the floor centrally and air flow direction towards the parking exit. Ventilation rates of 20, 40 and 60 m^3/min were simulated, which corresponded to 1.7, 3.5 and 5.2 air change per hour (ACH). Hydrogen release was simulated vertically downward, release opening 5×5 cm, hydrogen velocity chosen to provide constant release volume rate Q=0.655 and 1.310 m^3/min. The authors observed that for the studied flow rate the ventilation significantly affected the flammable cloud volume and practically eliminated it in both considered cases, which was attributed to a much larger ventilation rate than the hydrogen leakage.

Matsuura et al. [6] examined numerically the effect of ventilation velocity in a scaled model of semi-open hallway ($L \times W \times H$=2.9×0.74×1.22 m) aiming to devise a control system for the forced ventilation. One end of the hallway was completely open. A single hydrogen leak opening and a single roof vent had the same sizes, 0.15×0.30 m. Effect of vent location in the roof and hydrogen leak location in the floor for different release flow rates 1.18×10^{-4} - 9.44×10^{-4} m^3/s, extraction fan rates 2.32×10^{-2} - 6.97×10^{-1} m^3/s (ACH=32-958) and extraction fan operation pattern were studied. The authors demonstrated that

under the investigated conditions the location of mechanical ventilation opening and ventilation rate had a significant effect on hydrogen distribution and propagation through the enclosure. The larger ventilation rates imposed strong inflow from the open end of the studied hallway, which overcame hydrogen plume buoyancy and prevented hydrogen from rising to the roof leading to its propagation along the floor.

Two engineering models [7] were developed within the HyIndoor project to aid ventilation design for indoor hydrogen installations. The passive ventilation model [7] assumes hydrogen accumulation from a steady-state release in a stratified layer under the enclosure ceiling. The approach was validated against 48 small-scale experiments with natural/passive ventilation performed by CEA [8] on helium release in a small scale enclosure of size $H \times W \times D$=1.26×0.93×0.93 m with one vent located on a wall near the ceiling. The calculation procedure may also be adapted to find the volumetric flow rate of mechanical ventilation not to exceed the targeted maximum hydrogen concentration in the stratified layer for a given constant hydrogen release rate. The perfect mixing model [9] is based on the perfect mixing equation and assumes uniform hydrogen distribution through the entire enclosure. The model allows calculating the forced ventilation flow rate not to exceed the targeted maximum hydrogen concentration for a given steady-state hydrogen release rate.

Solutions for both the passive ventilation model [7] and the forced ventilation perfect mixing model [9] are based on two strong assumptions: (1) perfect mixing in the stratified layer and perfect mixing in the entire enclosure respectively, (2) steady-state formulation corresponding to the constant hydrogen release rate. Violation of each of the approaches leads to a decrease of the modelling results accuracy. Transient release of finite onboard storage inventory in a large enclosure, e.g. underground parking, is a real-life scenario leading to spatial and temporal distribution of hydrogen, i.e. violation of both assumptions simultaneously. Application of analytical models in this situation would not be justified and engineering solutions should employ more accurate technique like CFD analysis.

This study aims to scrutinise the effect of TPRD diameter and release direction of unignited hydrogen release in the context of underground parking and/or traffic systems, investigate the release interaction with typical for car parking mechanical ventilation, and propose the safety strategy for safe introduction of FCEV in underground infrastructure.

2.0 THE SIMILARITY LAW FOR ASSESSMENT OF UPWARD RELEASE

2.1 Safety strategy

The safety strategy for inherently safer FCEV underground parking is to eliminate the formation of a flammable cloud under the ceiling preventing the potential of its ignition and destructive deflagration. In the case of upward releases, the similarity law [10] can be used to calculate the TPRD diameter that would allow the jet decay below 4% by volume before reaching the ceiling. Hydrogen concentration decay along the centre-line of a free, unobstructed hydrogen jet can be described by fundamentally based and extensively validated for both expanded and underexpanded jets similarity law [10]:

$$\frac{C_{ax}}{C_N} = 5.4 \cdot \sqrt{\frac{\rho_N}{\rho_S}} \frac{D}{x}, \quad (1)$$

where x is the axial distance from the nozzle to the point of interest where concentration decays to concentration C_{ax} (m); D is the real nozzle exit diameter (m); C_{ax} is a mass fraction of hydrogen in air at axial distance x; C_N is hydrogen mass fraction in the nozzle ($C_N = 1.0$ for pure hydrogen release); ρ_N is the density at the real nozzle exit (kg/m^3); ρ_S is the ambient air density (kg/m^3). The similarity law was realised as one of the tools of e-Laboratory (fch2edu.eu/home/e-laboratory) developed within the project NET-Tools (https://www.h2fc-net.eu/).

A simple safety strategy may be based on the minimisation of release opening to provide hydrogen concentration decay below the flammability limit before the jet reaches the enclosure ceiling. Once hydrogen concentration under the ceiling is below the lower flammability limit (LFL), i.e. 4% vol. hydrogen, then formation and built-up of flammable hydrogen-air cloud there is excluded. The similarity law can be reformulated to provide distance along the jet axis to the location where hydrogen mass fraction reaches the specified value:

$$x = \frac{5.4 \times D}{C_{ax}} \cdot \sqrt{\frac{\rho_N}{\rho_S}}, \quad (2)$$

where x is the vertical distance between the release orifice (i.e. TPRD location) and the ceiling (m), and $C_{ax} = 0.00288$ is the hydrogen mass fraction corresponding to the hydrogen LFL (4% vol.).

2.2 Example of inherently safer TPRD diameter calculation

Consider a vehicle in underground parking with a ceiling height of 3.0 m. The vehicle onboard hydrogen storage pressure is 70 MPa. The storage is equipped with TPRD that is installed at a height 0.5 m above the floor and vents vertically upward. The surrounding temperature is 288 K. What TPRD diameter will obey the described above safety strategy to exclude the formation of a flammable layer under a ceiling? For that, the concentration on the jet axis at the ceiling should be below 4% by volume (corresponding mass fraction is C_{ax}=0.00288). For an unignited jet, the similarity law Eq.(1) tool of the e-Laboratory can be applied to calculate concentration on the jet axis. The location of the TPRD above the floor and the height of the ceiling must be taken into account for assessment. Procedure for calculations by hand [10]:

1. Calculate the pressure in the real nozzle exit as a function of the storage pressure:
   $P_N = \frac{P_R}{(\frac{\gamma+1}{2})^{\frac{\gamma}{\gamma-1}}} = \frac{70000000\ Pa}{(\frac{1.4+1}{2})^{\frac{1.4}{1.4-1}}} = 36979725$ Pa.
2. Calculate the Z factor using the Abel-Nobel equation of state for real gas:
   $Z = 1 + \frac{b \cdot P_R}{R_{H_2} \cdot T} = 1 + \frac{0.007691 \cdot 70000000\ Pa}{4124.24 \cdot 288\ K} = 1.4533.$
3. Calculate density of hydrogen in the real nozzle exit:
   $\rho_N = \frac{P_N}{Z \cdot R_{H_2} \cdot T} = \frac{36979725\ Pa}{1.4533 \cdot 4124.24\ J/K/kmol \cdot 288\ K} = 21.4226$ kg/m^3.
4. Calculate the maximum nozzle diameter sufficient to exclude the formation of flammable cloud using Eq.(2):
   $D = \frac{x}{5.4} \frac{C_{ax}}{C_N} \sqrt{\frac{\rho_S}{\rho_N}} = \frac{2.5\ m}{5.4} \frac{0.00288}{1} \sqrt{\frac{1.205\ \text{kg/m3}}{21.4226\ \text{kg/m3}}} = 0.000316\ m = 0.3$ mm.

This is a quite small diameter of TPRD and care should be taken that it is sufficient for blowdown from the tank in a fire to exclude the tank rupture.

3.0 NUMERICAL STUDY OF DOWNWARD RELEASE FROM TPRD

3.1 The CFD model details

In this study, we look into the example of a real underground car park in St. Martnes Latem (Gent, Belgium) [11]. The top view of the car park with dimensions is given in Figure 1. The car park height is 3.0 m, the total parking area is A=1115 m^2. The onboard hydrogen storage with the volume of 62.4 L, storage pressure 70 MPa, initial temperature 288 K and several TPRD diameters were studied.

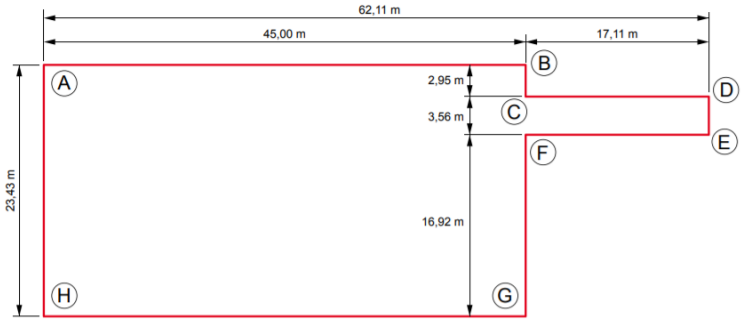

Figure 1. Underground car park layout (St. Martnes Latem, Gent, Belgium) [10].

The transient problem formulation using ANSYS FLUENT 20R is considered to account for the blowdown of the storage tank. The pressure-based implicit solver and the second-order upwind scheme selected for the momentum, species, energy equations and equations of the realizable k-ε turbulence model [12]. The calculation domain and numerical mesh are shown in Figure 2. The calculation domain

included the underground parking itself and part of the tunnel entrance (section BDEF in Figure 1). The numerical grids consisted of 440k poly-hex-core control volumes uniformly distributed inside the calculation domain and refined at the release zone. The inflow boundary for the fresh air is shown in Figure 2 by the blue arrow and the outflow boundary of ventilation extraction openings are designated by red arrows and resolved as 6x6 cells each.

Details of 15 numerical tests are presented in Table 1. Hydrogen releases from TPRD of diameter 0.5 mm, 0.75 mm, 1 mm and 2 mm were simulated. The effects of ventilation, release diameter and angle, ceiling height and presence of an obstacle in a form of a wall behind the vehicle were investigated. In simulations with mechanical ventilation in accordance with BS BS 7346-7:2013 [4], the extraction outflow was modelled to provide 10 ACH and was arranged in evenly distributed over the ceiling extraction vents (18 vents, 1x1 m each). The boundary was set as uniform outflow velocity in the vent area. Outflow velocity was calculated based on the specified 10 ACH as 33450 m^3/h /60 min=557 m^3/min /60 s =9.28 m^3/min / 18 m^2 =0.516 m/s. FCEV was positioned close to the car park centre as demonstrated in Fig. 2 except for simulations No. 12 and 13, where it was positioned back to the wall.

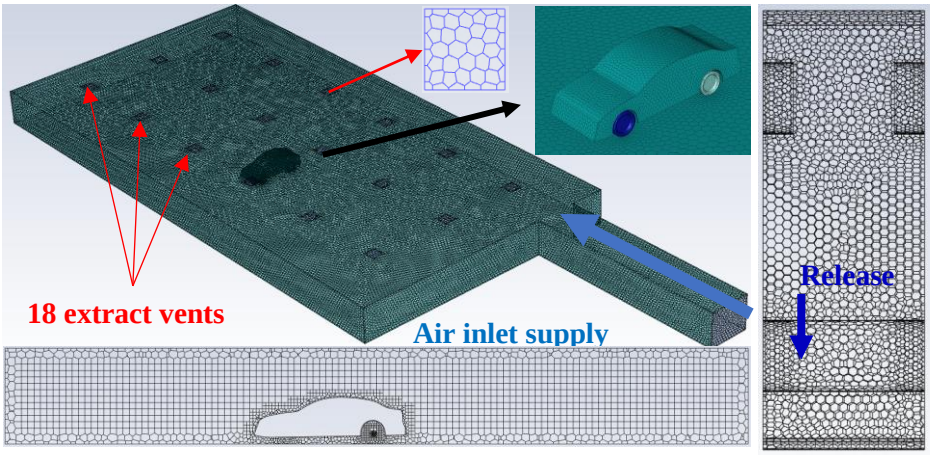

Figure 2. Calculation domain and numerical grid.

Table 1. Details of 15 numerical tests with hydrogen release.

No.	$\varnothing_{TPRD}$, mm	ACH	Angle, °	Obstacle	Ceiling height, m
1	0.5	0	45	-	3.0
2	0.5	10	45	-	3.0
3	0.5	10	0	-	3.0
4	0.5	10	30	-	3.0
5	0.5	10	60	-	3.0
6	0.75	10	30	-	3.0
7	0.75	10	0	-	3.0
8	0.75	10	45	-	3.0
9	1.0	10	45	-	3.0
10	2.0	10	45	-	3.0
11	0.75	0	45	-	2.1
12	0.5	0	45	Wall	2.1
13	0.75	0	45	Wall	2.1
14	0.75	0	45	-	3.0
15	0.75	10	45	-	2.1

3.2 Blowdown simulations

The volumetric source technique [10] was applied to simulate the blowdown release for all 15 scenarios. For each selected nozzle diameter the changing with time hydrogen mass flow rate, velocity, temperature, turbulence model parameters at the notional nozzle were modelled applying source terms

in corresponding equations. The dynamics of storage pressure, mass flow rate, temperature and velocity in the nozzle are shown in Figure 3. Turbulence intensity in the notional nozzle was chosen according to [13] as $TI = 25\%$, turbulence length scale as $TLS = 0.07 d_{not}$, where d_{not} is the diameter of the notional nozzle calculated following [10]. The area of volumetric source term application was modelled according to [10, 14] as a cube with the side area equal to the area of the maximum notional nozzle at the start of the release was resolved by 2x2x2 hexahedral cube cells (see Table 2), located on the left hand side of the vehicle 12 cm from the inner side of the wheel (as shown in Fig. 2 by blue arrow). The volume of the source term was kept constant.

Table 2. Volumetric source parameters used in CFD simulations.

$\varnothing_{TPRD}$, mm	Storage P, MPa	Storage T, K	l_{VS} side, mm	V_{VS}, m^3	Cell size, mm
0.5	70	288	7.47	$4.16 \cdot 10^{-07}$	3.74
0.75			11.2	$1.41 \cdot 10^{-06}$	5.6
1.0			14.9	$3.33 \cdot 10^{-06}$	7.45
2.0			29.9	$2.67 \cdot 10^{-05}$	14.95

The source terms were calculated as follows:

- mass conservation equation source term: $S_{mass} = \frac{\dot{m}_{H_2}}{V_{vs}}$,
- momentum conservation equation source term: $S_{mom} = \frac{u_{H_2} \cdot \dot{m}_{H_2}}{V_{vs}}$, where u_{H2} is the notional nozzle velocity,
- turbulent kinetic energy conservation equation source term: $S_\kappa = \frac{\kappa \cdot \dot{m}_{H_2}}{V_{vs}}$,
- dissipation of turbulent kinetic energy source term: $S_\varepsilon = \frac{\varepsilon \cdot \dot{m}_{H_2}}{V_{vs}}$,
- energy conservation equation source term: $S_E = \frac{c_{p,H_2} \cdot (T_{H_2} - T_0) \cdot \dot{m}_{H_2}}{V_{vs}}$, where T_{H2} is the notional nozzle temperature,
- turbulent kinetic energy: $\kappa = \frac{3}{2}(u_{H_2} \cdot TI)^2$,
- dissipation rate of turbulent kinetic energy: $\varepsilon = 0.0845^{0.75} \frac{\kappa^{1.5}}{TLS}$.

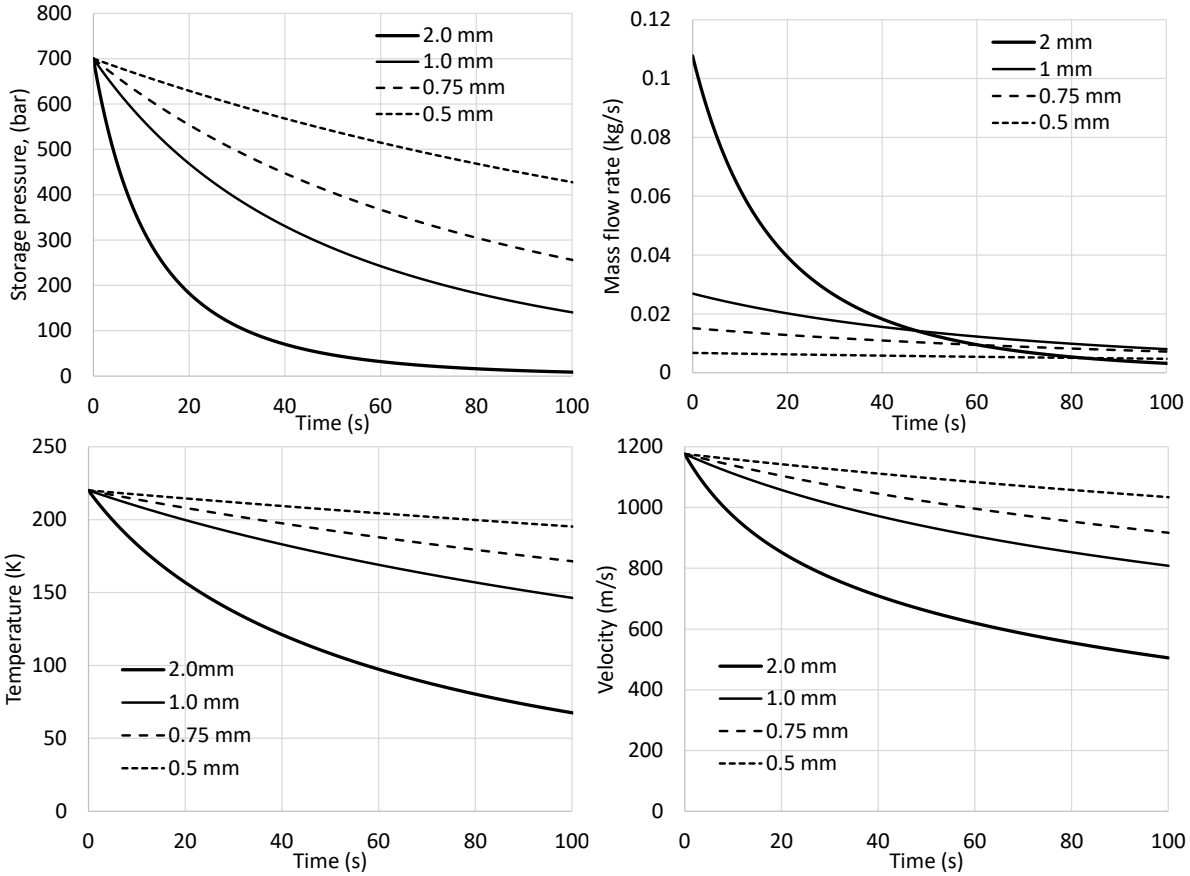

Figure 3. Initial stage of dynamics of storage pressure, mass flow rate, notional nozzle temperature and velocity during the blowdown.

4.0 RESULTS AND DISCUSSION

4.1 Effect of mechanical ventilation

The simulations were performed with ACH=0 and ACH=10 to assess the effect of ventilation on the formation of the flammable layer under the ceiling and estimate the hazard distance based on the flammable envelope distance to LFL. Figure 4 shows simulation results for TPRD ∅0.5 and TRPD ∅0.75 mm for the case of 3 m ceiling height and TPRD ∅0.75 mm for 2.1 m ceiling height (the ventilation velocity was reduced proportionally to the volume to fulfil 10 ACH); in all demonstrated cases TPRD release was directed at the angle A=45° to the vertical. The shown snapshots are for the moments when the longest hazard distance during the blowdown release of hydrogen is observed. Figure 4 demonstrates that there is no visible effect of regulated mechanical ventilation on the hazard distance. This is thought due to higher velocities of hydrogen jet compared to air velocity and the comparatively short time when the jet reaches its maximum size during the blowdown process. Figure 4 shows as well that hydrogen concentration decays below 4% without reaching the ceiling, thus no accumulation of hydrogen and flammable mixture formation under the ceiling is expected.

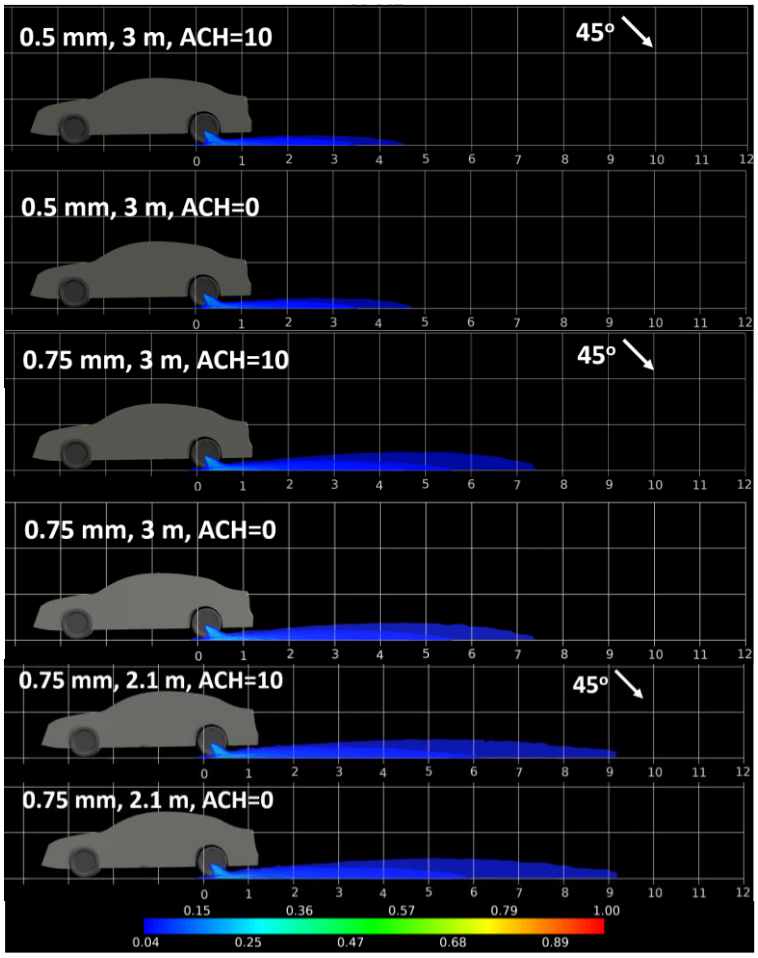

Figure 4. Effect of ventilation (ACH=10) versus no ventilation (ACH=0) on hydrogen flammable envelope: TPRD ∅0.5 mm, 3.0 m ceiling (top); TPRD ∅0.75 mm, 3.0 m ceiling (middle); TPRD ∅0.75 mm, 2.1 m ceiling (bottom), A=45°.

The semi-transparent blue colour contour in Figure 4 shows the iso-surface of 4% by volume of hydrogen in the air as a maximum distance in any direction, while the next grade of blue shows 4% decay across the centre-plane. It can be seen that in all cases the distance defined by the iso-surface is larger than the distance in the centre-plane. This is due to the shift of TPRD location as can bee seen from Fig. 2 from the vehicle axis, and hence the wheel prevents additional intraiment into the jet during the impingement and attachment of hydrogen jet at the floor. This can be seen in Fig. 5, which shows top view of the flammable envelope for the case of TPRD ∅0.75 mm, release at the angle A=45° to the vertical, ceiling heights 2.1 and 3.0, with and without ventilation at time t=7 s. It should be noted that for the case with ACH=10 the width of the flammable envelope is wider compared to ACH=0.

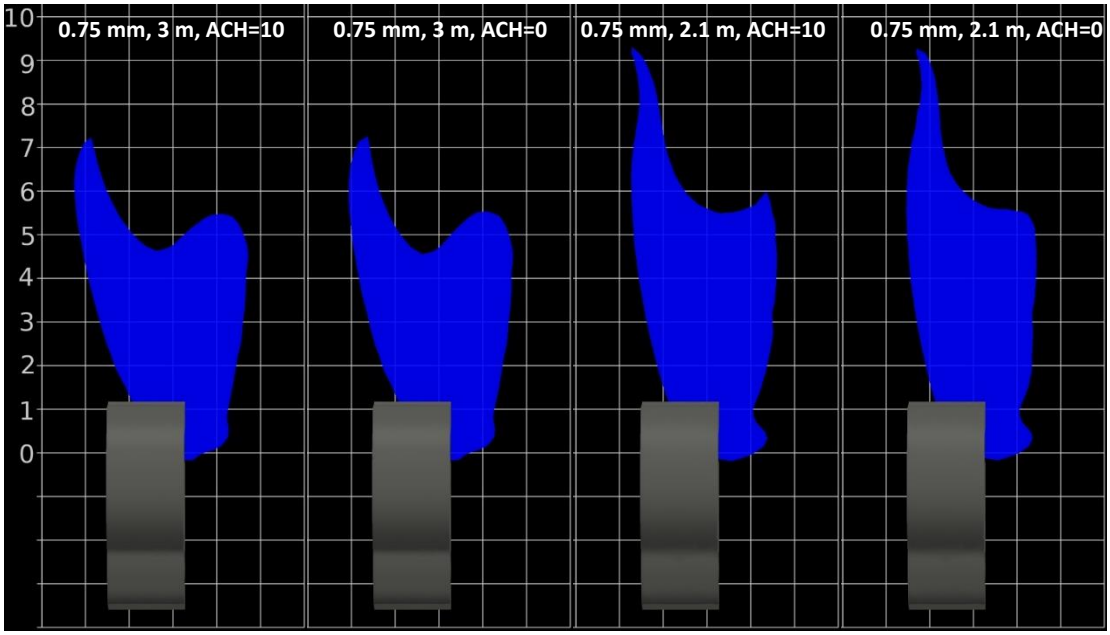

Figure 5. Flammable envelope shape: TPRD ∅0.75 mm, A=45º, 2.1 and 3 m ceiling, ACH=0 and 10 at time *t*=7 s.

Figure 6 shows dynamics of maximum horizontal distance of flammable envelope propagation from the release point in simulations No. 1-11, 14 and 15. Figure 6 (left) for TPRD ∅0.5 mm and angle A=45º demonstrates that the larger is the angle of release from the vertical axis the larger is the hazard distance. The maximum hazard distance is only marginally (3.5%) decreased by the ventilation. Figure 6 (right) shows horizontal maximum hazard distance for larger TPRD diameters in the range 0.75-2.0 mm. It reaches its maximum within 4-10 s and then gradually decreases due to blowdown. For TPRD ∅0.75 mm, A=45º and heights 2.1 and 3.0 m the effect of ventilation is practically indistinguishable.

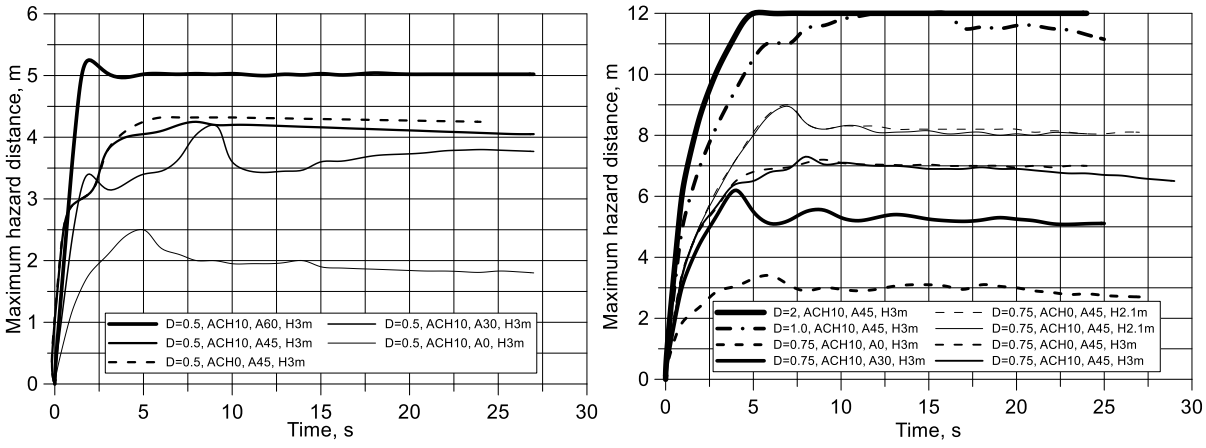

Figure 6. Dynamics of maximum flammable envelop propagation in the presence and absence of ventilation and for different release angles. Left: TPRD ∅0.5 mm. Right: TPRD ∅0.75-2.0 mm (including different ceiling heights).

4.2 Effect of the ceiling height

The effect of the ceiling height is demonstrated in Figure 4 (middle and bottom) where the largest flammable envelopes are compared for 3.0 m and 2.1 m ceilings for the same TPRD ∅0.75 mm, both with and without ventilation. It can be seen that for the lower ceiling the largest flammable envelope propagation distance is about 2.0 m longer (25%) which presumably is due to the different entrainment of air caused by a 30% reduction of the height. Figure 6 shows that this difference is reached at about time *t*=6.0-6.5 s. The difference gradually decreases with time and stabilises at about 1.0 m (12%) after

time *t*=12 s. As it was demonstrated in Fig.5 the maximum distance of flammable envelop propagation was achieved not on the jet axis, but at its periphery.

4.3 Effect of TPRD release angle

Simulations No.2-8 (TPRD ∅0.5 mm and 0.75 mm, ACH=10, ceiling height 3.0 m) were used to assess the effect of TPRD release direction which varied between A=0° and 60° on the flammable envelope propagation. Figure 7 shows the flammable envelopes at the moment they reach their maximum size in each particular simulation. For both investigated TPRD diameters the increase of the angle consistently increased the maximum hazard distance (no simulation for A=60º and TPRD ∅0.75 mm was performed as the LFL propagation distance in this case would be even further).

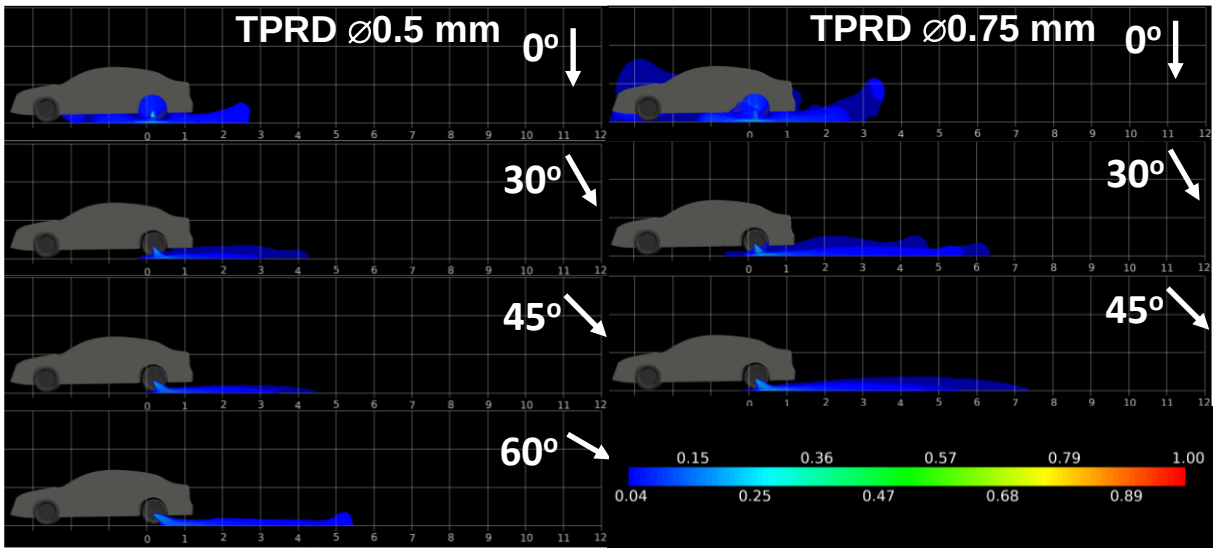

Figure 7. Effect of release angle: hydrogen mole fraction (flammable envelope distance to 4%), 3.0 m ceiling height, ACH=10, TPRD ∅0.5 mm (left), TPRD ∅0.75 mm (right).

Releases at A=0º and 30º produced shorter flammable envelop distances compare to releases at A=45º for both release diameters, however they created large flammable spots underneath the car towards the front and side passenger doors threatening passengers evacuation in case of ignited release. Additionally, releases at angle A=30º resulted in a thicker flammable envelope compared to A=45° in both simulations, TPRD ∅0.5 and ∅0.75 mm.

Figure 8 shows that releases vertically down (at angle A=0°) are capable to form buoyant flammable clouds which can accumulate under the ceiling even with active mechanical ventilation (ACH=10).

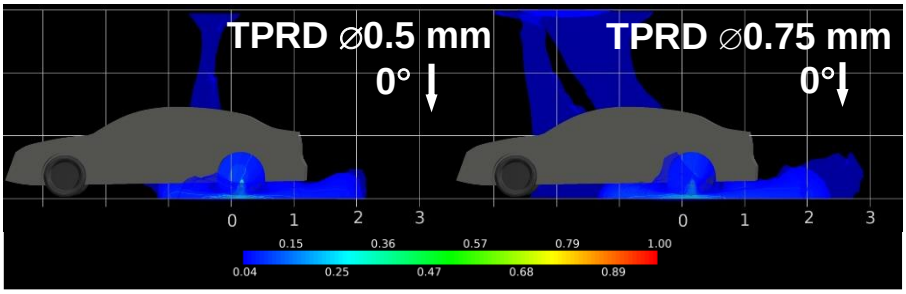

Figure 8. Downward releases at 30 s from TPRD ∅0.5 mm (left), ∅0.75 (right), A=0º, ACH=10.

For the above reasons only releases at the angle A=45º will be analysed further.

4.4 Effect of TPRD diameter

Effect of TPRD diameter on flammable cloud shape is demonstrated in Figure 9 using simulations No. 2,
8, 9, 10 (release angle A=45°, ceiling height 3.0 m). The figure shows flammable envelopes created by releases from different TPRDs at the time *t*=6 s when the flammable composition from TPRD ∅2.0 mm reaches the ceiling and starts to form the flammable layer. Flammable compositions for TPRD ∅0.5, 0.75 and 1.0 mm decay a long time before the jet propagation is affected by buoyancy preventing flammable cloud formation under the ceiling. In the considered parking area the release from TPRD ∅2.0 mm appears the most hazardous: its flammable envelop not only the longest one, but, after losing its momentum due to interaction with the wall, threatens with accumulation of substantial hydrogen-air cloud.

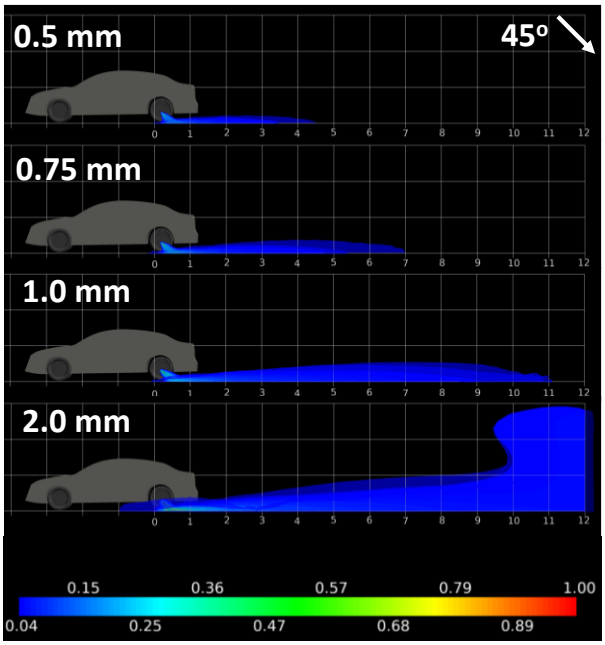

Figure 9. Effect of TPRD diameter on flammable envelope propagation, A=45°, ACH=10.

4.5 Effect of obstruction in absence of ventilation (worst case)

Simulations No. 12 and 13 (TPRD ∅0.5 and ∅0.75 mm, angle A=45°) were performed to assess the worst-case scenario of FCEV located in a parking space next to a wall, under a low ceiling (height 2.1 m) and in absence of ventilation (ACH=0). TPRD release was directed towards the wall, the distance between the wall and FCEV bumper was 0.2 m. Figure 10 shows flammable hydrogen-air mixture propagation at the time *t*=8 s for ∅0.5 and t=11 s for ∅0.75 mm. Simulations demonstrate that currently the formation of flammable cloud cannot be avoided even in the case of the smallest considered TPRD ∅0.5 and ∅0.75 mm when FCEV is parked next to a wall. It is recommended to avoid parking the vehicle with TPRD directed towards the obstruction.

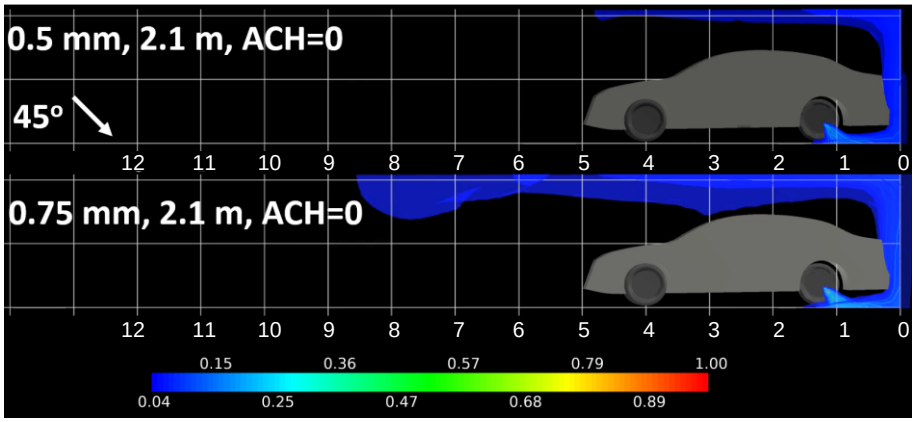

Figure 10. Effect of obstacle on flammable cloud formation TPRD ∅0.5 mm (top) and ∅0.75 mm (bottom), A=45°, ACH=0.

4.6 Mass of flammable hydrogen and potential overpressure hazards in case of ignition

Pressure hazards of potential hydrogen-air cloud deflagration were studied using an available analytical model for a localised mixture deflagration in a closed vessel [15]. The model is based on a number of assumptions: perfectly sealed enclosure (no openings to provide deflagration venting); localised hydrogen-air mixture occupies only portion of the enclosure, but has uniformly distributed hydrogen within the mixture at LFL 4% vol. (which provides the largest deflagration overpressure for a given hydrogen mass); complete combustion. The analysis performed in [15] concluded that to avoid deflagration overpressure above 10 kPa, which is a typical limit for integrity of civil structures, the hydrogen inventory in the enclosure should not be larger than $m_{H2} = 2.61 \cdot 10^{-4}\, V$, where m_{H2} is the mass of hydrogen (kg) and V is the volume of the enclosure (m^3).

The studied car parking has a volume of 3,345 m^3. Application of the above analysis to the considered car park means that to reach uniform across the whole parking overpressure 10 kPa the mixed with air hydrogen mass should be $m_{H2} = 2.61 \cdot 10^{-4} \cdot 3345 = 0.873$ kg. In reality, the deflagration of this hydrogen mass would result in lower than 10 kPa overpressure because: (1) the parking is not perfectly sealed and has openings at least in form of extraction ventilation and entrance gate, and (2) any deviation of real mixture hydrogen content from assumed in the model uniform 4% vol. composition (with fixed total hydrogen mass) decreases resultant overpressure.

Figure 11 shows the dynamics of hydrogen-air cloud mass in the parking for all studied release scenarios. Figure 11 (left) gives dynamics of hydrogen mass within the flammability limits (4-74% vol. hydrogen). The maximum hydrogen mass reaches ca. 0.38 kg for release from the largest TPRD ∅2.0 mm, ACH=10, release angle A=45°. This is significantly lower than the analytical limit of 0.873 kg leading to the conclusion that deflagration of hydrogen releases from lesser than TPRD ∅2.0 mm diameter will not result in overpressures threatening structural integrity.

Releases from smaller TPRDs results in a further decrease of hydrogen mass within the flammability limits. The least flammable hydrogen mass is observed, naturally, for TPR ∅0.5 mm – here maximum hydrogen mass is about 27g (A=0°) which is 14 times smaller compare to about 380 g for TPRD ∅2.0 mm (A=45°). Increase of release angle from A=0° to 60° for TPRD ∅0.5 mm decreases flammable hydrogen mass further down to just 4 g – nearly 7 times.

A fast-burning hydrogen-air mixture with close to stoichiometry composition may provide large overpressure in a nearfield. To have insight into these potential hazards the obtained simulation results are compared to the experimental program with near stoichiometric hydrogen-air deflagrations in hemispherical clouds performed at Fraunhofer ICT [16]. In the experiments, the smallest volume of stoichiometric hydrogen-air mixture of 7.5 m^3 (0.19 kg hydrogen) generated for open atmosphere unobstructed deflagration the nearfield peak overpressure of 3.4 kPa.

Figure 11 (right) shows hydrogen mass in the fastest burning (and the most hazardous for overpressure generation) composition 25-35%. The largest hydrogen mass of just 1.55 g was registered for release from TPRD ∅2.0 mm. This corresponds to 0.062 m^3 volume of stoichiometric hydrogen-air mixture at 29.5% vol. hydrogen. Therefore a preliminary conclusion may be drawn that for all simulated release cases the combustion of the fast-burning near-stoichiometric mixture should not create overpressure

above 3.4 kPa which is not capable to cause any damage to structures (in absence of obstructions leading to flame acceleration).

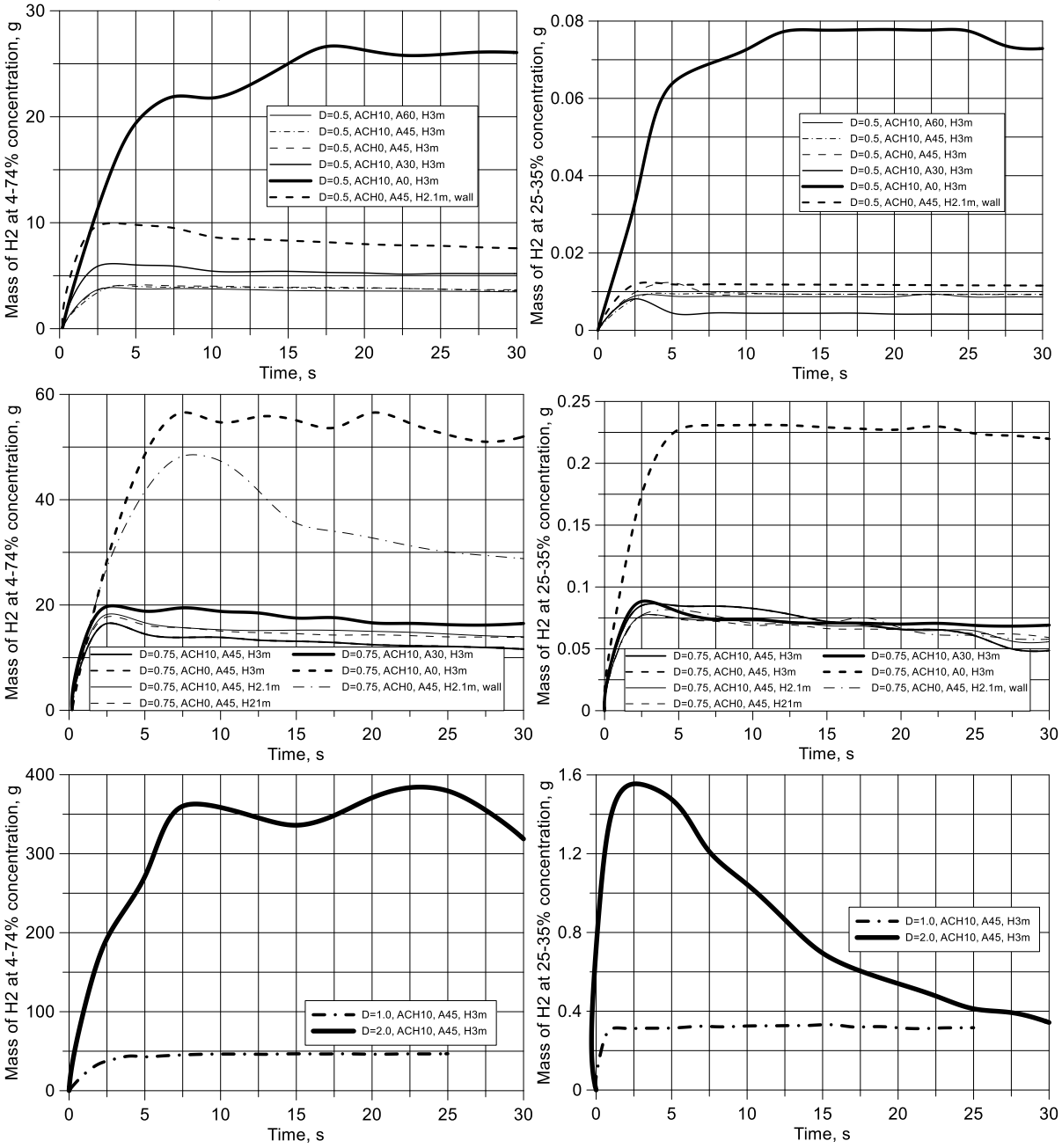

Figure 11. Dynamics of flammable mass of hydrogen: within flammability limits 4-74% vol. (left), within fastest burning composition 25-35% vol. (right); TPRD ∅0.5 mm (top), ∅0.75 mm (middle), ∅2.0 mm (bottom).

5.0 CONCLUSIONS

The *originality* of the performed research is in conducting analysis of hydrogen release and dispersion from a high-pressure hydrogen tank in an underground parking taking into account the effect of release direction, angle, ceiling height and ventilation. Safety strategy based on similarity law for concentration decay along hydrogen jet axis and allowing to exclude flammable mixture formation under car parking ceiling by limiting TPRD diameter is demonstrated for vertical release direction. The series of 15 simulations of unignited blowdown releases taking into account realistic vehicle and car parking geometry with and without account of mechanical ventilation in underground parking is performed providing detailed information on hydrogen-air mixture dynamics.

The *rigour* of this work is in the consistent and detailed analysis across the whole range of potential TPRD design parameters (diameter, release direction), realistic car park geometries (heights, space), ventilation rates (from no ventilation, ACH=0, up to regulated 10 ACH).

The s*ignificance* of this study is in demonstrating that the proper design of TPRD deem to satisfy safety requirements in case of accidental hydrogen release in underground car parking which mechanical ventilation is compliant with currently existing RCS. The fact enables the use of currently existing parking and underground infrastructure with the new generation of FCEV. To underpin the safe introduction of FCEV into underground infrastructure the following conclusions were drawn:

- The general strategy for underground parking is to eliminate the formation of flammable cloud under the ceiling.
- For the upward releases, the similarity law can be used to calculate at what TPRD size the hydrogen jet will decay below 4% before reaching the ceiling.
- The ventilation does not affect on hydrogen flammable clouds formed by releases from TPRD ∅0.5-0.75 mm.
- TPRD release direction at the angle A=45° deem to be the overall best safety solution. Releases at the angle A=0° generate buoyant hydrogen-air plume and forming flammable layer under the ceiling. Releases at the angle A=0° and 30° provide mixture propagation toward the front and rear wheels, which, if ignited, will contradict to RCS requirements for FCEV.
- Releases from TPRD ∅0.5 and ∅0.75 mm don't result in a flammable layer formation under car park ceiling for the considered range of ceiling heights (2.1-3.0 m) and ventilation rates - ACH=0 (no ventilation) and ACH=10 (required mechanical ventilation rate in case of fire).
- Releases from TPRDs with a diameter above 0.75 mm have the potential to create a flammable layer, especially in the absence of mechanical ventilation.
- Releases from TPRD toward obstacles tend to prohibit hydrogen mixing with air and promote accumulation of a flammable cloud; it should be recommended not to park FCEV with TPRD directed towards obstruction.
- The use of analytical models for analysis of mechanical ventilation effect on hydrogen propagation from onboard storage releases deem to suffer loss of accuracy due to transient and highly non-uniform hydrogen distribution. This is particularly pronounced for enclosures with large volume and complex geometries. The use of more accurate methods capable to resolve spatial and temporal hydrogen dynamics like CFD should be considered for these problems.

The above discussion has the potential to provide a valuable contribution to the recommendations to regulations, codes and standards (RCS) related to dealing with unignited hydrogen releases in confined spaces.

6.0 ACKNOWLEDGEMENTS

The authors are grateful to Engineering and Physical Sciences Research Council (EPSRC) of the UK for funding this work through SUPERGEN Hydrogen and Fuel Cell Hub project (EP/P024807/1), and the HyTunnel-CS and SH2APED projects have received funding from the FCH2 JU under grant agreements No.826193 and No.101007182. This Joint Undertaking receives support from the European Union's Horizon 2020 research and innovation programme, Hydrogen Europe and Hydrogen Europe Research.

7.0 REFERENCES

1. IEC 60079-10-1, International Electrotechnical Commission IEC 60079-10-1, Explosive atmospheres - Part 10-1: Classification of areas - Explosive gas atmospheres, 2015.
2. NFPA 2, National fire protection association NFPA 2, Hydrogen technologies code, 2011.
3. ISO/DIS 19880-1, 19880-1 TI organization for standardization I, Gaseous hydrogen – fuelling stations, Part 1: General requirements, 2018.
4. British Standard institution BS 7346-7:2013. Components for smoke and heat control systems – Part 7: Code of practice on functional recommendations and calculation methods for smoke and heat control systems for covered car parks 2013.
5. Choi, J., Hur, N., Kang, S., Lee, E. and Lee, K., A CFD simulation of hydrogen dispersion for the hydrogen leakage from a fuel cell vehicle in an underground parking garage, *Int J Hydrog Energy*, **38**, 2013, https://doi.org/10.1016/j.ijhydene.2013.02.018.

6. Matsuura, K., Nakano, M. and Ishimoto, J., Forced ventilation for sensing-based risk mitigation of leaking hydrogen in a partially open space, *Int J Hydrog Energy*, **35**, 4776–86, 2010, https://doi.org/10.1016/j.ijhydene.2010.02.068.
7. Molkov, V., Shentsov, V. and Quintiere, J., Passive ventilation of a sustained gaseous release in an enclosure with one vent, *Int J Hydrog Energy*, **39**, 8158–68, 2014, https://doi.org/10.1016/j.ijhydene.2014.03.069.
8. Cariteau B, Tkatschenko I. Experimental study of the effects of vent geometry on the dispersion of a buoyant gas in a small enclosure. *Int J Hydrog Energy*, **38**, 8030–8, 2013, https://doi.org/10.1016/j.ijhydene.2013.03.100.
9. Adams P, Bengaouer A, Cariteau B, Molkov V, Venetsanos AG. Allowable hydrogen permeation rate from road vehicles. *Int J Hydrog Energy*, **36**, 2742–9, 2011, https://doi.org/10.1016/j.ijhydene.2010.04.161.
10. Molkov, V., Fundamentals of Hydrogen Safety Engineering. www.bookboon.com, free download book, 2012.
11. ArcelorMittal. Underground car parks n.d. https://projects.arcelormittal.com/repository/Unassigned/Docs/Case%20studies/carparks.pdf
12. Shih, T.-H., Liou, W.W., Shabbir, A., Yang, Z., and Zhu, J. A New Eddy-Viscosity Model for High Reynolds Number Turbulent Flows - Model Development and Validation, *Computers Fluids.*, **24**(3), 227–238, 1995, https://doi.org/10.1016/0045-7930(94)00032-T
13. Brennan, S. L., Makarov, D. V., and Molkov, V., LES of high pressure hydrogen jet fire, *J. Loss Prev. Process Ind.*, 22, no. 3, 353–359, May 2009, https://10.1016/j.jlp.2008.12.007.
14. Molkov, V., Makarov, D., and Bragin, M., Physics and modelling of under-expanded jets and hydrogen dispersion in atmosphere, in *Proceedings of the 24th International Conference on Interaction of Intense Energy Fluxes with Matter*, Elbrus, Chernogolovka, 2009, pp. 143–145, ISBN 978-5-901675-89-2.
15. Makarov, D., Hooker, P., Kuznetsov, M. and Molkov, V., Deflagrations of localised homogeneous and inhomogeneous hydrogen-air mixtures in enclosures, *Int J Hydrog Energy*, **43**, 9848–69, 2018, https://doi.org/10.1016/j.ijhydene.2018.03.159.
16. Schneider H., Pförtner H. Fraunhofer-institut fur treib-und explosivstoffe. ICTProjektforschung 19/83. Forschungsprogramm “Prozeßgasfreisetzung - Explosion in der Gasfabrik und Auswirkungen von Druckwellen auf das Containment”. Ballonversuche zur Untersuchung der Deflagration von Wasserstoff/Luft-Gemischen (Abschlußbericht), 1983.